Materials Science and Engineering B 159–160 (2009) 70–73

Contents lists available at ScienceDirect

Materials Science and Engineering B

journal homepage: www.elsevier.com/locate/mseb

Silicon nanostructures for solar cell applications

F. Gourbilleau[a,*], C. Dufour[a], B. Rezgui[b], G. Brémond[b]

[a] CIMAP, UMR CNRS/CEA/Ensicaen 6252, 6 Bd Maréchal Juin, 14050 Caen Cedex, France
[b] INL, UMR CNRS 5270, Université de Lyon, INSA-Lyon, Bat. Blaise Pascal, 7 Av. Jean Capelle, 69621 Villeurbanne Cedex, France

ARTICLE INFO

Article history:
Received 30 April 2008
Received in revised form 20 October 2008
Accepted 24 October 2008

Keywords:
Si nanostructure
Si-rich/SiO_2 superlattice
Photovoltaic
Reactive magnetron sputtering

ABSTRACT

Among the numerous applications of Si nanostructures in the microelectronic or photonic domains, one which could be promising concerns the use of such structures as the active layer in pin solar cells. By taking advantage of the quantum confinement of the carriers in Si nanograins whose size is lower than 8 nm, it is expected to improve the solar cell efficiency by increasing the absorption range of the solar spectrum. In this work, we report the fabrication, microstructural and optical properties of Si-rich silicon oxide (SRSO) composite layers and SRSO/SiO_2 multilayers fabricated by reactive magnetron sputtering process. This process allows monitoring either the Si nanograins size and/or the Si nanograin density through specific deposition parameters such as the hydrogen rate in the plasma, the substrate temperature, the annealing treatment. Their effects on the photoluminescent properties as well as on the absorption coefficient are discussed. The SRSO/SiO_2 multilayers absorption is higher with respect to the SRSO composite layer. Such behaviour has been attributed to a better control of the Si nanograin size.

1. Introduction

The discovery of the quantum confinement effect in silicon grain having a size smaller than 8 nm has opened the way of the optoelectronic field to nanostructured Si-based devices. Thus numerous studies dealing with the efficient visible photoluminescence (PL) at room temperature (RT) from Si nanograins (Si-ng) have been reported [1–9] and more recently the efficient sensitizing role played by Si-ng towards rare earth ions has been clearly demonstrated [10–13]. Such systems are now subject of deep investigations. Concerning the photovoltaic applications, they are closely linked to the development of the third generation of solar cells. This new generation aims at reducing the cost per Watt by increasing drastically the efficiency of the solar cell [14]. One of the proposed routes consists in the fabrication of nanostructured cells from abundant and non-toxic materials such as silicon, using low-dimensional structures like quantum wires (QW), quantum dots taking advantage of the widening of absorption spectrum in the UV range [15]. Another way consists in doping the up-converting layer by rare earth ions [16].

To widen the absorption spectrum of a solar cell, Conibeer et al. [15] propose to use the tandem cells approach allowing to stack different layers having different energy thresholds. In such an approach, the upper cell is constituted of nanostructured Si-based materials which are suitable to engineer the bandgap. The main challenge consists in managing the presence of an insulating SiO_2 host matrix allowing the quantum confinement of carriers in Si nanograins with the achievement of carrier mobility in the whole cell. Different ways are investigated such as N-doped SiO_2 or SiC matrices to reduce and control the bandgap. Another approach consists in using Si-rich–SiO_2 (SRSO)/SiO_2 superlattice structures in which the quantum confinement is monitored through the thickness of the Si-rich sublayer whereas the carrier injection can be improved by controlling the thickness of the SiO_2 sublayer [7,8].

In this paper, we describe the optical properties of SRSO and SRSO/SiO_2 layers fabricated by reactive magnetron sputtering of a pure silica target with hydrogen-rich Ar plasma. By this original approach, the Si nanograins size and density are controlled through specific deposition parameters and their effects on the optical properties are analyzed.

2. Experimental

Thick (~1 μm thick) SRSO composite layers and SRSO/SiO_2 multilayers were deposited by reactive magnetron co-sputtering of a pure SiO_2 target. In both cases, the silicon excess in the layer is obtained through the monitoring of the hydrogen rate r_H ($r_H = P_{H_2}/P_{H_2} + P_{Ar}$). This reactive deposition approach is based on the ability of hydrogen to react with oxygen species issue from the sputtering of the SiO_2 target. Such a reactive approach allows the control of Si incorporation in the grown thin film [17]. The films are deposited on quartz and Si substrates maintained at

* Corresponding author. Tel.: +33 231452656; fax: +33 231452660.
E-mail address: fabrice.gourbilleau@ensicaen.fr (F. Gourbilleau).

0921-5107/$ – see front matter © 2008 Elsevier B.V. All rights reserved.
doi:10.1016/j.mseb.2008.10.052

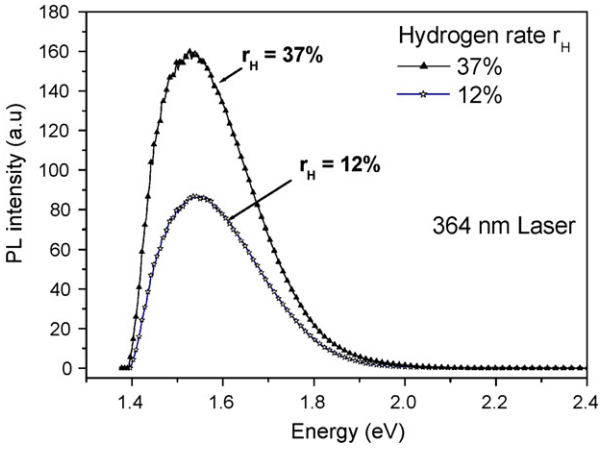

Fig. 1. PL spectra of composite layers deposited with r_H = 12% and r_H = 37% under a 364 nm excitation line.

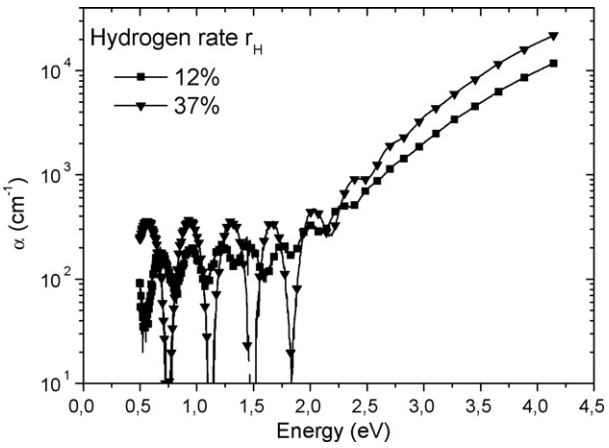

Fig. 2. Absorption coefficient as a function of the energy for composite layers deposited with r_H = 12% and r_H = 37%.

600 °C for the multilayers and 60 °C for the composite layers. The RF power applied during the growth is fixed to 0.76 W cm^{-2}. After deposition, the films are submitted to an annealing treatment at 1100 °C during 60 min under a N_2 flux in order to favour the Si–SiO_2 phase separation and to allow the photoluminescence analysis thanks to the recovery of the trap charge defects.

Microstructural characterizations are performed by means of high-resolution electron microscopy (HREM) in a cross sectional approach leading to the observations of the layer in the growth direction. The optical properties have been investigated by means of room temperature (RT) photoluminescence (PL) measurements using a 488, 364 and 244 nm excitation wavelengths of an Ar Laser. The optical transmission experiments were performed between 0.5 and 4.1 eV using a double beam PerkinElmer (l9) spectrophotometer.

3. Results and discussion

3.1. Composite SRSO layers

Fig. 1 reports the photoluminescence (PL) spectra recorded on two SRSO composite layers deposited with two different hydrogen rates, r_H = 12 and 37%. The comparison of the PL emission recorded under a 364 nm laser excitation shows an increase of the peak intensity for the composite layer fabricated with the highest hydrogen rate while the maximum PL position for both layers remains the same, peaking at about 1.54 eV. Such a behaviour means that both layers contain a similar Si-ng size population whose mean value is roughly estimated to about 5 nm by applying the empirical relation proposed by Delerue et al. [18]. This large value is attributed to the fact that this relation has been determined for free Si nanocrystals and not Si-ng embedded in a SiO_2 host matrix. The high difference in the PL intensity for films having the same Si-ng size distribution indicates that the increase of the hydrogen partial pressure in the plasma, i.e. r_H, favours the incorporation of the Si excess leading to the formation of a higher Si-ng density. Experiments on the microstructure are under progress to confirm this analysis and to correlate these PL results with the effect of the deposition parameters. The corresponding absorption spectra are reported in Fig. 2 in the 0.5–4.5 eV range. Before 2 eV, the oscillations are coming from reflections occurring between the film and the substrate due to the thickness of the deposited layers which is close to 1.4 μm. The comparison of the two curves shows that the composite layer deposited with the highest hydrogen rate has a highest absorption coefficient than the one fabricated with r_H = 12%. Such a difference could be linked to the highest density of the Si-ng as deduced from the PL experiments.

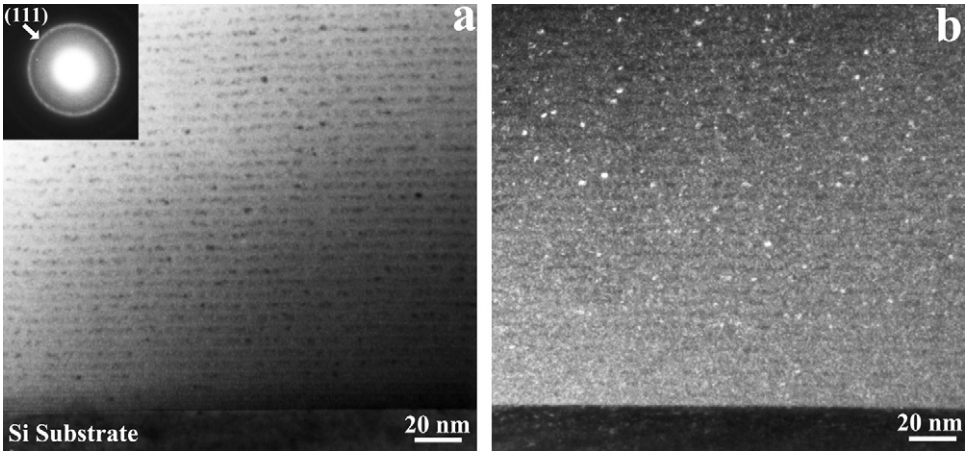

Fig. 3. TEM micrographs of a typical SRSO/SiO_2 multilayer with a 3 nm thick SRSO and 3 nm thick SiO_2 sublayers (a) in a bright field approach; (b) in a dark field approach using the (1 1 1) diffraction.

3.2. SRSO/SiO_2 multilayers

Two sets of multilayers (MLs) have been fabricated in which the number of sublayers has been fixed to have almost the same SRSO "thickness" allowing the comparison of the films. Thus MLs are constituted either of 165 or 300 SRSO/SiO_2 patterns with a SRSO sublayer thickness of 6 and 3 nm, respectively. For both MLs, the thickness of the silica sublayer has been fixed at 3 nm. A typical micrograph of such MLs is presented in Fig. 3 and consists here of a 3 nm thick SRSO/3 nm thick SiO_2 stacking. One can notice the regular stacking of each sublayer (Fig. 3a). The corresponding electron diffraction pattern evidences the presence of Si nanocrystallites in the SRSO layers as revealed by the (1 1 1) ring. By selecting some (1 1 1) diffraction spots, the dark field imaging clearly demonstrates the presence of Si nanocrystals in the SRSO sublayer. The PL experiments performed with a 488 nm Ar excitation line are reported in the inset of Fig. 4. One can observe the presence of large emission band usually reported for the Si-ng emission, peaking at about 1.5 eV. The intensity of the layer containing the thinnest SRSO sublayers is five times higher than the 6 nm-thick SRSO ML after normalization to the total SRSO thickness. The shape of the emission spectrum changes when the MLs are excited under a 244 nm line due to the excitation in the direct band gap of the Si-ng (Fig. 4). Shoulders appear on both spectra but at two different energies and the maximum peak position is slightly shifted. Thus, the Gaussian fits evidences the presence of three emission bands peaking at 1.47, 1.58 and 2.22 eV, whereas, in the case of the thinner SRSO ML, the emission bands are found to peak at 1.54, 1.7 and 2.22 eV. This later PL peak is present for both MLs and is attributed to the presence of defects in the oxide. Concerning the two other PL peaks, a previous work [19] performed on similar MLs has shown their presence and has linked them to the interface Si/SiO_2. The consequence is an emission at about 1.5 eV and Si-ng size dependent quantum confinement effect. Consequently, the emission bands peaking at 1.47 and 1.7 eV observed on the MLs PL spectra can be correlated to the Si-ng size fixed by the SRSO sublayer thickness, 6 and 3 nm, respectively. The evolution of the absorption coefficient as a function of the energy for these two MLs is reported in Fig. 5. The MLs constituted of the thicker SRSO sublayer, i.e. the larger Si nanograin, present a higher absorption in the whole range of energy. The comparison of the absorption between composite or multi-layers reveals an increase of α by at least a factor 4 depending on the energy: as an example at 2.38 eV, for the composite layer $\alpha = 525\ cm^{-1}$ whereas in the case of the MLs, α reaches $2933\ cm^{-1}$. Such a result corresponds to a better control of the silica thickness as well as on the Si-ng size in the multilayer configuration.

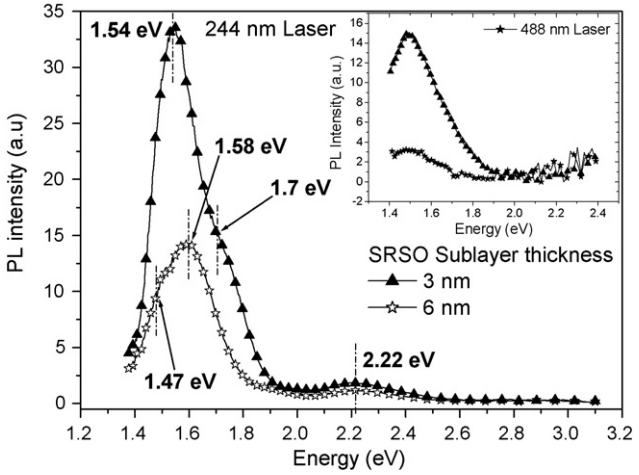

Fig. 4. PL spectra of multilayers with 3 and 6 nm thick SRSO sublayers under a 244 nm excitation line. In inset PL spectra recorded under a 488 nm Ar laser excitation line are shown.

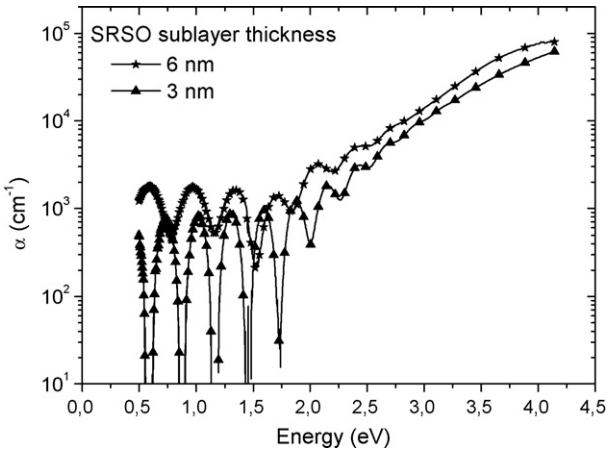

Fig. 5. Absorption coefficient as a function of the energy for mutlilayers [6 nm SRSO/3 nm SiO_2] × 165 and [3 nm SRSO/3 nm SiO_2] × 300.

4. Conclusion

The formation of nanocrystalline Si grains embedded in SRSO films grown using reactive magnetron sputtering process were investigated. The control of the silicon nanocrystal size and density as well as the absorption coefficient has been demonstrated using photoluminescence and optical transmission measurements. We have concluded that the PL process of Si nanocrystals combines two radiative transitions coming from quantum confinement effect in the Si nanocrystals and from the interfacial region between the grain and the surrounding host matrix. This opens the way to further investigations with the aim of developing high efficiency silicon-based third generation solar cells with such a material approach.

Acknowledgment

This work was supported by the Agence National de la Recherche (ANR) through the "*Cellules photovoltaïques tandem tout silicium*" DUOSIL project (ANR-06-PSPV-005).

References

[1] L.T. Cahnam, Appl. Phys. Lett. 57 (1990) 1046.
[2] Y. Kanemitsu, T. Ogawa, K. Shiraishi, K. Takeda, Phys. Rev. B 48 (1993) 4883.
[3] F. Priolo, S. Coffa, G. Franzo, C. Spinella, A. Carrera, V. Bellani, J. Appl. Phys. 74 (1993) 4936.
[4] Z.H. Lu, D.J. Lockwood, J.M. Baribeau, Nature 378 (1995) 258.
[5] L.S. Liao, X.M. Bao, X.Q. Zheng, N.S. Li, N.B. Min, Appl. Phys. Lett. 68 (1996) 850.
[6] L. Rebohle, J. Von Borany, W. Skorupa, I.E. Tyschenko, H. Fröb, J. Lumin. 80 (1999) 275.
[7] F. Gourbilleau, X. Portier, C. Ternon, P. Voivenel, R. Madelon, R. Rizk, Appl. Phys. Lett. 78 (2001) 3058.
[8] M. Zacharias, J. Heitmann, R. Scholtz, U. Kahlere, M. Schmidt, J. Blasing, Appl. Phys. Lett. 80 (2002) 661.
[9] A. Belarouci, F. Gourbilleau, Appl. Phys. B 88 (2007) 237;
A.J. Kenyon, P.F. Trwoga, M. Federighi, C.W. Pitt, J. Phys. Condens. Matter 6 (1994) L319.
[10] M. Fujii, K. Imakita, K. Watanabe, S. Hayashi, J. Appl. Phys. 84 (1998) 4525.
[11] G. Franzò, S. Bonelli, D. Pacifici, F. Priolo, F. Iacona, C. Bongiorno, Appl. Phys. Lett. 82 (2003) 3871.
[12] F. Gourbilleau, L. Levalois, C. Dufour, J. Vicens, R. Rizk, J. Appl. Phys. 95 (2004) 3717.

[13] D. Pacifici, L. Lanzanò, G. Franzò, F. Priolo, F. Iacona, Phys. Rev. B 72 (2005), 045349-1.
[14] M.A. Green, Third Generation Photovoltaics: Ultra-High Efficiency at Low Cost, Springer–Verlag, 2003.
[15] G. Conibeer, M. Green, R. Corkish, Y. Cho, E.-C. Cho, C.-W. Jiang, T. Fangsuwannarak, E. Pink, Y. Huang, T. Puzzer, T. Trupke, B. Richards, A. Shalav, K.-L. Lin, Thin Solid Films 511–512 (2006) 654.
[16] A. Shalav, B.S. Richards, T. Trupke, K.W. Krämer, H.U. Güdel, Appl. Phys. Lett. 86 (2005) 031505.
[17] C. Ternon, F. Gourbilleau, X. Portier, P. Voivenel, C. Dufour, Thin Solid Films 419 (2002) 5.
[18] C. Delerue, G. Allan, M. Lanoo, Phys. Rev. B 48 (1993) 11024.
[19] C. Ternon, F. Gourbilleau, R. Rizk, C. Dufour, Physica E 16 (2003) 517.